Progress In Electromagnetics Research Letters, Vol. 52, 105–112, 2015

Design and Analysis of a Controllable Miniaturized Triband Frequency Selective Surface

Huangyan Li and Qunsheng Cao*

Abstract—A novel miniaturized combined-element frequency selective surface (CEFSS) with simple design process is proposed for multiband applications. In this article, complementary meandered structures and complementary grid structures are combined to realize controllable tri-band characteristics, which allow the designed FSS to transmit different frequency signals at 3.3, 4.5 and 5.4 GHz while reflecting signals at 4.0 and 4.9 GHz. The miniaturized combined-element FSS in this paper has the advantage of smaller size comparing to traditional tri-band FSSs due to the use of meandered structures, which contributes to its independence of both angle and polarization. The associated equivalent circuit is provided to analyze its transmission characteristics. Furthermore, the performances of the proposed structure are evaluated by simulation and measurement, and they agree well.

1. INTRODUCTION

Frequency selective surfaces (FSSs) are able to transmit desired signals while reflecting unnecessary signals. FSSs, as a kind of spatial filters, are widely used in sub-reflectors, radomes and many other fields [1].

For practical applications, the FSSs are often required to have multiband characteristics by enabling transmission in several desired frequency bands. Recently, many methods have been used to realize multiband characteristics of FSSs. Ref. [2] proposed a dual-band FSS that is fulfilled by placing two different square loops in one period. A tri-band FSS was designed by combining rings with different radiuses [3]. In [4], the complementary structures were mentioned to have a dual-band characteristic with two transmission poles and one transmission zero. However, in many cases, sizes of FSSs are required to be small enough because of the limited areas and the need to delay grating lobes.

In [5], a miniaturization design was proposed by using bending metal strips. Lumped components were used to design miniaturized FSSs [6]. In [7] complementary meander lines were adopted to realize a miniaturized dual-band FSS.

In [8], combined-elements were adopted to form a tri-band FSS. However, the separation between the first and the latter two transmission poles is limited above a certain value, which undermines the controllability of this structure in those applications requiring narrower stopband between two adjacent passbands.

To improve the controllability of this structure, complementary meandered structures and complementary grid structures are combined in this paper. By replacing complementary square loops with complementary meandered structures, the latter two passbands can be tuned to a lower frequency band than before. Equivalent circuit is applied to fully analyze and explain this structure's filter mechanism. To verify the validity of this design, a prototype with transmission poles at 3.3, 4.5 and 5.4 GHz is fabricated and measured, and the measuring results agree well with the simulation results.

Received 18 December 2014, Accepted 5 February 2015, Scheduled 29 March 2015

* Corresponding author: Qunsheng Cao (qunsheng@nuaa.edu.cn).

The authors are with the College of Electronic and Information Engineering, Nanjing University of Aeronautics and Astronautics, Nanjing 210016, China.

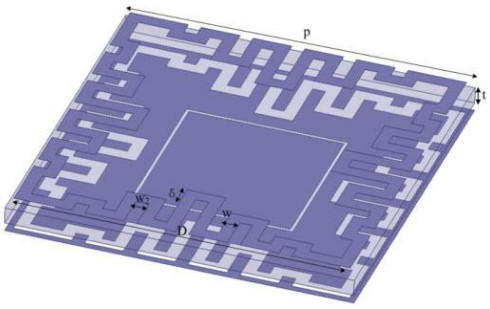

Figure 1. Combined structure of the complementary meandered structures and the single square aperture structure.

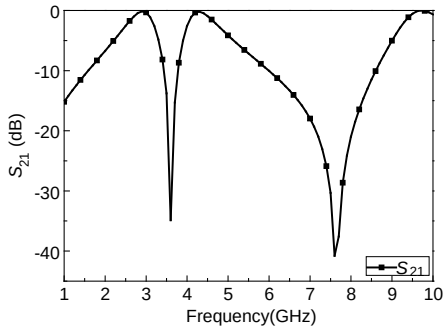

Figure 2. Transmission response of the complementary meandered structures and the single square aperture structure.

Table 1. Detailed physical parameters of the first combined-element FSS (unit: mm).

Parameter	l	s	D	g	w	w_2	δ	t
Value	5.7	0.2	10.8	0.4	0.4	0.4	0.7	0.8

Table 2. Detailed physical parameters of the second combined-element FSS (unit: mm).

Parameter	p	g_1	D	g	w	w_2	δ	t
Value	11	0.4	9.3	0.4	0.4	0.4	0.7	0.8

2. DESIGN AND ANALYSIS OF THE PROPOSED STRUCTURES

2.1. Basic Design of the Combined-Element FSS

Table 1 gives the detailed physical parameters of the combined-element FSS as shown in Figure 1. Using the commercial full-wave finite element method (FEM) simulator Ansoft HFSS, the combined structure has the transmission property shown in Figure 2. It has three transmission poles at 2.9, 4.3 and 9.7 GHz and two transmission zeros at 3.6 and 7.6 GHz.

The transmission poles at 2.9 and 4.3 GHz are introduced by the complementary meandered structures, while the transmission pole at 9.7 GHz is introduced by the single square aperture. Particularly, the additional transmission zero at 7.6 GHz is introduced by the coupling of the two structures after combination, which improves the frequency selectivity of the combined structure.

However, the size of single square aperture is restricted to the meandered aperture. Therefore, the corresponding transmission pole introduced by the single square aperture can't move to a lower frequency band independently.

2.2. Design of a New Combined-Element FSS

In order to control the extra transmission pole in a lower frequency band independently, a novel miniaturized structure is proposed.

2.2.1. Geometry of the Proposed FSS

This combined structure, of which the top consists of the wire grid and the meandered loop and the bottom layer is composed of the wire aperture and the meandered aperture, is shown in Figure 3. The detailed geometry parameters are listed in Table 2 ($\varepsilon_r = 2.65$).

The simulated transmission curve from HFSS of this combined-element FSS in Figure 4 shows that the transmission property of this novel structure is the simple combination of the properties of the complementary meandered structures and the complementary grid structures. There are three transmission poles at 3.3, 4.5 and 5.4 GHz and two transmission zeros at 4.0 and 4.9 GHz, respectively. The transmission poles at 4.5 and 5.4 GHz are introduced by the complementary meandered structures and the transmission pole at 3.3 GHz is introduced by the complementary grid structures. Particularly,

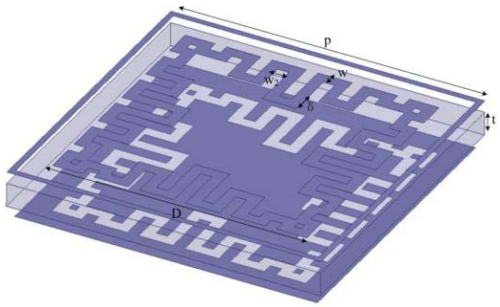

Figure 3. Combined structure of the complementary meandered structures and the stacked wire grid and aperture grid structure.

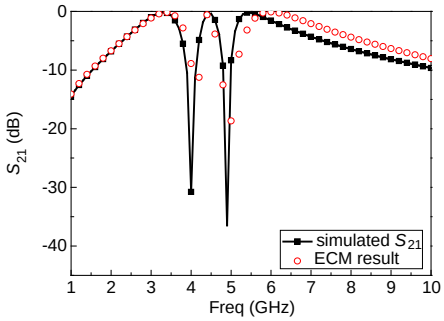

Figure 4. Transmission response of the complementary meandered structures and stacked wire grid and aperture grid.

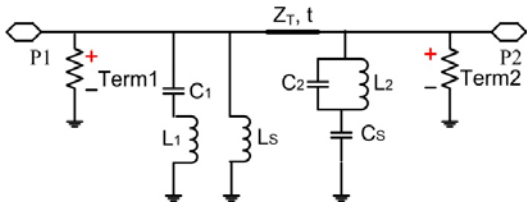

Figure 5. Equivalent circuit of the combined-element structure.

the additional transmission zero at 4.0 GHz is introduced by the coupling of the two structures after combination, which improves the frequency selectivity of the combined structure. And a slight shift of the transmission curve can be observed after the combination because of the couplings among structures.

2.2.2. Equivalent Circuit Analysis

The combined-element FSS can also be analyzed qualitatively with equivalent circuit method [9–11]. As shown in the equivalent circuit in Figure 5, the meandered loop and its complementary structure can be equivalent to a series resonant circuit (L_1, C_1) and a parallel resonant circuit (L_2, C_2), respectively. Meanwhile, the wire grid structure can be equivalent to the inductance L_s parallel to the series LC resonant circuit while the aperture grid structure can be equivalent to the capacitance C_s in series with the parallel LC resonant circuit. The free space at both sides of the combined-element FSS is modeled as transmission lines with a characteristic impedance of $Z = 377\,\Omega$. The dielectric substrate supporting this structure can be considered as a short transmission line with a length of t and its wave impedance is $Z_T = Z_0/\sqrt{\varepsilon_r}$. The equivalent impedance of this combined-element FSS is derivedas in Eq. (1).

$$Z = \frac{\dfrac{[j\omega L_1 + 1/(j\omega C_1)]\, j\omega L_s}{j\omega L_1 + 1/(j\omega C_1) + j\omega L_s} \left\{ \dfrac{j\omega L_2 [1/(j\omega C_2)]}{j\omega L_2 + 1/(j\omega C_2)} + \dfrac{1}{j\omega C_s} \right\}}{\dfrac{[j\omega L_1 + 1/(j\omega C_1)]\, j\omega L_s}{j\omega L_1 + 1/(j\omega C_1) + j\omega L_s} + \dfrac{j\omega L_2 [1/(j\omega C_2)]}{j\omega L_2 + 1/(j\omega C_2)} + \dfrac{1}{j\omega C_s}} \tag{1}$$

and it can be simplified as:

$$Z = \frac{j\omega L_s \left(1 - C_1 L_1 \omega^2\right) \left[1 - (C_2 + C_s) L_2 \omega^2\right]}{-A\omega^6 + B\omega^4 - C\omega^2 + 1} = \frac{jL_s (1/\omega - C_1 L_1 \omega) [1/\omega - (C_2 + C_s) L_2 \omega]}{-A\omega^3 + 1/\omega^3 + B\omega - C/\omega} \tag{2}$$

where

$$A = C_1 C_2 C_s L_1 L_2 L_s$$
$$B = L_1 L_2 C_1 C_2 + L_2 L_s C_1 C_2 + L_1 L_2 C_1 C_s + L_2 L_s C_1 C_s + L_1 L_s C_1 C_s + L_2 L_s C_2 C_s$$
$$C = (L_1 C_1 + L_2 C_2 + L_2 C_s + L_s C_1 + L_s C_s)$$

From Formula (2), it is easy to find that Z has two zeros and three poles, which agrees with the result shown in Figure 4. The focus here in this paper is on the transmission pole associated with the complementary wired lines, which satisfies the following formula [8]:

$$f_{pass1} \approx \frac{1}{2\pi\sqrt{L_s C_s + \varepsilon_0 \varepsilon_r t/2}} \tag{3}$$

The relationship between the equivalent inductance L_s and equivalent capacitor C_s and the physical parameters of the proposed structure is provided as follows [12]:

$$L_s = \mu_0 \left(p/2\pi\right) \log\left[\csc\left(\pi\omega/2p\right)\right] \tag{4}$$

$$C_s = \varepsilon_0 \varepsilon_{eff} \left(2l/\pi\right) \log\left[\csc\left(\pi s/2l\right)\right] \tag{5}$$

where p and w are the period and the width of the wire grid structure, l and s are the side length of the conducting patch and the width of the gap between two patches. The approximate value of the effective permittivity of the structure is:

$$\varepsilon_{eff} \approx \left(1 + \varepsilon_r\right)/2 \tag{6}$$

Choose the parameters in Table 2, then $p = 11\,\text{mm}$, $w = g_1/2 = 0.2\,\text{mm}$, $l = p - g_1 = 10.6\,\text{mm}$ and $s = g_1 = 0.4\,\text{mm}$. The effect of the tiny transmission line can be neglected since the height of the substrate is very small, so the approximate value of the frequency point of the first transmission pole we obtain from Formulas (3)–(6) is about 3.27 GHz, which is close to the simulated result 3.30 GHz shown in Figure 4. Although there's a 30 MHz difference between the two results because the effects of transmission line and mutual couplings of components are not taken into consideration, we still can make primary design of the first transmission pole independently and quickly without the use of commercial softwares.

The transmission curve from the equivalent circuit method based on ADS is also plotted in Figure 4, which agrees well with the simulated result.

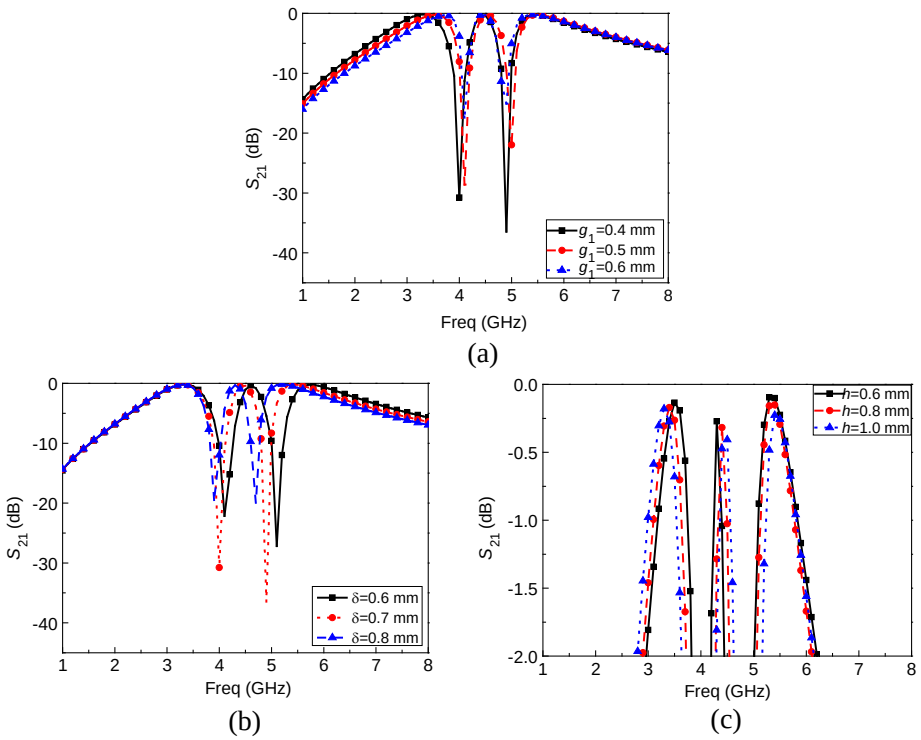

Figure 6. Simulated transmission responses of the proposed FSS with different parameters, (a) g_1; (b) δ; (c) h.

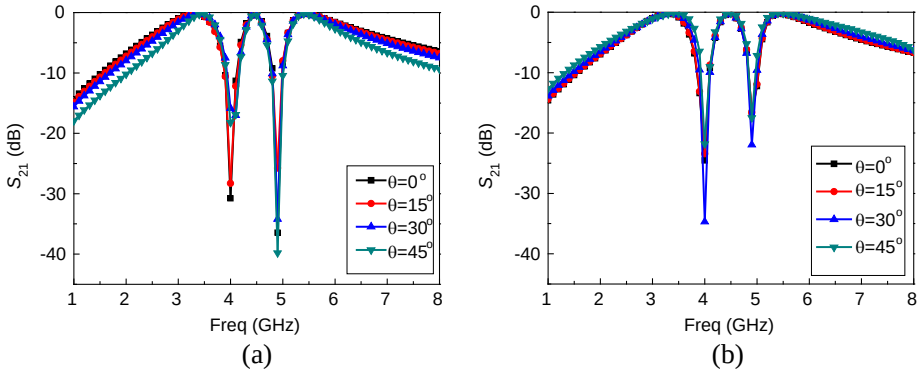

Figure 7. Simulated transmission responses of the proposed FSS with different θ and polarization model, (a) TE; (b) TM.

From the analysis above, this combined-element FSS provides three transmission poles and two transmission zeros, which improves the frequency selective characteristics and can be applied in many fields of multiband systems. The size of this combined-element FSS is reduced to about $\lambda_{pass1}/10$ due to the introduction of miniaturized structure, which ensures better angular stability and polarization stability than traditional FSSs.

2.2.3. Parameter Analysis

The effects of the main geometry parameters of the proposed combined-element FSS on transmission poles and zeros are shown in Figure 6, including the width of the wire grid g_1, the increasing level of the meander line δ and the height of the substrate h. The value of the equivalent capacitance C_s decreases as g_1 increases, so the center frequency point of the first passband increases as can be seen in Eq. (3), which agrees with the simulation result shown in Figure 6(a). The smaller the value of δ is, the smaller the difference between the meandered structure and the single square aperture structure, and the miniaturization degree becomes less obvious, which agrees with the simulation result shown in Figure 6(b).

As seen in Figure 6(c), the insertion loss increase as the height of the substrate increases. In this study, a substrate with the height of 0.8 mm is adopted considering the commercial availability in fabrication.

Figure 7(a) and Figure 7(b) show the transmission curves of this combined-element structure under the incident plane wave with different incident angles (θ) and polarization states. The transmission characteristics of this combined-element FSS is relatively stable to the variations of both incident angle and polarization state.

3. ANALYSIS OF CASCADED FSSS

As discussed above, the proposed tri-band combined-element FSS has the advantages of miniaturization and stable frequency performance. However, it is necessary to further study high-order FSSs. High-order FSSs are often designed based on cascading technique. Two combined-element FSSs shown in Figure 3 are cascaded with an air spacing of 15 mm and its equivalent circuit model is shown in Figure 8. Figure 9 plots its simulated transmission curve compared with that of the single FSS. As we can see, the operating frequencies of the two situations agree well while the cascaded structure provides sharper transmission curve than that of the single FSS. Thus, the frequency selective characteristics are improved significantly.

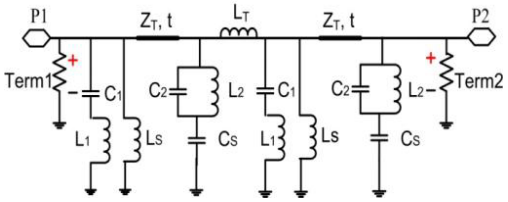

Figure 8. Equivalent circuit model of the cascaded FSSs.

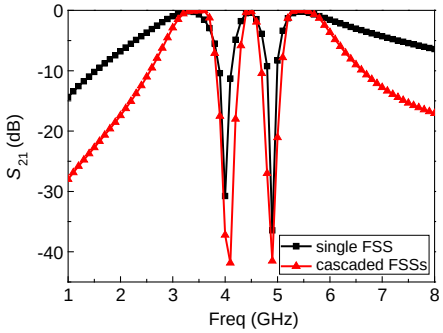

Figure 9. Simulated transmission responses of cascaded structure compared with that of single FSS.

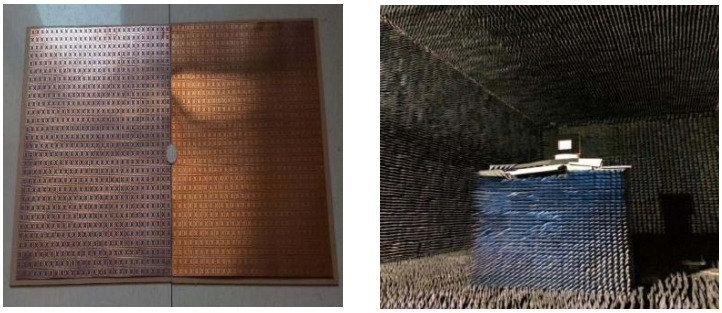

(a) (b)

Figure 10. (a) Both sides of the FSS prototype; (b) set-up in the microwave anechoic chamber.

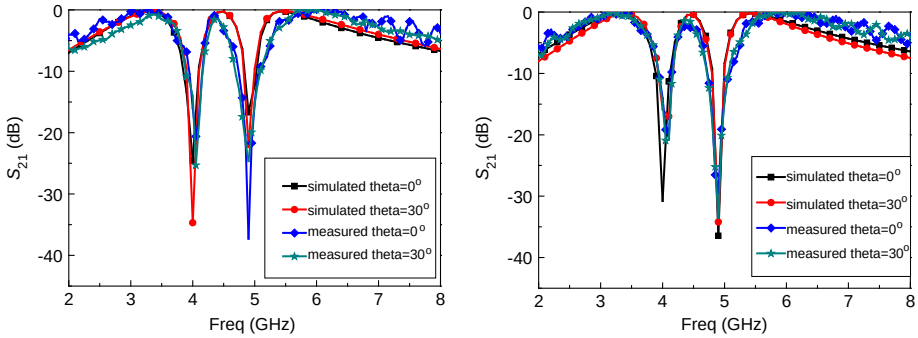

(a) (b)

Figure 11. Measured transmission responses of the combined-element structure under different incident angles, (a) TE mode; (b) TM mode.

4. EXPERIMENTAL VERIFICATION

A prototype of the combined-element is fabricated and measured to demonstrate the validity of the proposed structure. The proposed structure is designed to transmit the signals at 3.3, 4.5 and 5.4 GHz while reflecting the signals at 4.0 and 4.9 GHz. Figure 10(a) shows the FSS prototype with 29×29 cells and a overall dimension of $319 \times 319\,\text{mm}^2$, fabricated on a 0.8 mm thick dielectric substrate with the permittivity of 2.65 and the loss tangent of 0.005, using a standard printed circuit board (PCB). The detailed design parameters are listed in Table 2. The measurement is carried out in a microwave

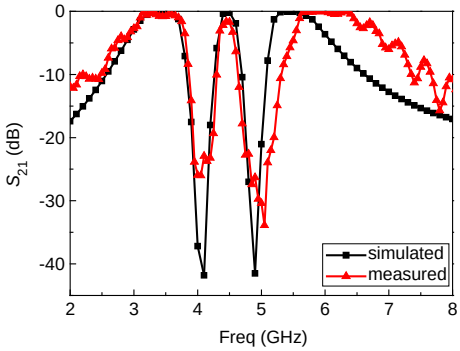

Figure 12. Measured transmission responses of the cascaded structure.

anechoic chamber as shown in Figure 10(b).

Transmission responses of full-wave simulations and measurements for different incident angles under different polarizations are plotted in Figures 11(a) and (b), and only a little deviation can be observed. The shift of the measured operating frequency can be attributed to the inaccuracy of fabrication and permittivity of the substrate. However, the measured result agrees well with the simulation in general. Figure 12 shows both the simulated and measured results of the cascaded structure, which proves that the cascaded structure has an abrupt falling down characteristic and a wider bandwidth than that of a single FSS.

5. CONCLUSION

A miniaturized combined-element FSS with three transmission poles and two transmission zeros is proposed based on the complementary structures. The effect of some important parameters on the transmission properties has been analyzed by full-wave simulation and a stable frequency response of the proposed structure with different incident angles and polarization modes is observed. The equivalent circuit method is carried out to fully analyze this structure. A prototype of this structure is fabricated for demonstration, and the measurement results agree well with the simulation ones. Furthermore, two proposed FSS structures are cascaded together to achieve a higherorder frequency selectivity.

ACKNOWLEDGMENT

This work has been supported by the project No. NBG0030113-1 funded by Nanjing industry-university-research cooperative innovation of Jiangsu Province science and technology plan project.

REFERENCES

1. Munk, B. A., *Frequency Selective Surfaces: Theory and Design,* Wiley, New York, 2005.
2. Pirhadi, A., F. Keshmiri, M. Hakkak, and M. Tayarani, "Analysis and design of dual band high directive EBG resonator antenna using square loop FSS as superstrate layer," *Progress In Electromagnetics Research*, Vol. 70, 1–20, 2007.
3. Huang, J., T. K. Wu, and S. W. Lee, "Tri-band frequency selective surface with circular ring elements," *IEEE Transactions on Antennas and Propagation*, Vol. 42, No. 2, 166–175, 1994.
4. Wang, D., W. Chen, Y. Chang, et al., "Combined-element frequency selective surfaces with multiple transmission poles and zeros," *IET Microwaves, Antennas and Propagation*, Vol. 8, No. 3, 186–193, 2014.
5. Yang, G., T. Zhang, W. Li, et al., "A novel stable miniaturized frequency selective surface," *IEEE Antennas and Wireless Propagation Letters*, Vol. 9, 1018–1021, 2010.

6. Liu, H. L., K. L. Ford, and R. J. Langley, "Design methodology for a miniaturized frequency selective surface using lumped reactive components," *IEEE Transactions on Antennas and Propagation*, Vol. 57, No. 9, 2732–2738, 2009.
7. Hu, X. D., X. L. Zhou, L. S. Wu, et al., "A miniaturized dual-band frequency selective surface (FSS) with closed loop and its complementary pattern," *IEEE Antennas and Wireless Propagation Letters*, Vol. 8, 1374–1377, 2009.
8. Wang, D., W. Che, Y. Chang, et al., "A low-profile frequency selective surface with controllable triband characteristics," *IEEE Antennas and Wireless Propagation Letters*, Vol. 12, 468–471, 2013.
9. Wang, H. Q., "Analysis of double band properties of frequency selective surfaces by using equivalent circuit method," *Systems Engineering and Electronics*, Vol. 30, No. 11, 2054–2057, 2008.
10. Cui, Y., X. Y. Hou, and C. K. Tang, "Equivalent-circuit for analysis of performance of double-square-loop FSS," *Journal of Missile and Guidance*, Vol. 26, No. 2, 322–324, 2006.
11. Li, X. L., P. C. Zhao, and Z. Y. Zong, "Equivalent circuit model for frequency selective surface loaded with lumped capacitance," *Journal of Nanjing University of Science and Technology*, Vol. 35, No. 4, 539–542, 2011.
12. Bayatpur, F., "Metamaterial-inspired frequency-selective surfaces," Ph.D. Dissertation, The University of Michigan, 2009.